

E. Berkenwald, M. L. Laganá, P. Acuña, G. Morales* and D. Estenoz*

Bulk Polymerization of Styrene using Multifunctional Initiators in a Batch Reactor: A Comprehensive Mathematical Model

DOI 10.1515/ijcre-2015-0102

Abstract: A detailed, comprehensive mathematical model for bulk polymerization of styrene using multifunctional initiators – both linear and cyclic – in a batch reactor was developed. The model is based on a kinetic mechanism that considers thermal initiation and chemical initiation by sequential decomposition of labile groups, propagation, transfer to monomer, termination by combination and re-initiation reactions due to undecomposed labile groups. The model predicts the evolution of global reaction variables (e.g. concentration of reagents, products, radical species and labile groups) as well as the evolution of the detailed complete polymer molecular weight distributions, with polymer species characterized by chain length and number of undecomposed labile groups. The mathematical model was adjusted and validated using experimental data for various peroxide-type multifunctional initiators: diethyl ketone triperoxide (DEKTP, cyclic trifunctional), pinacolone diperoxide (PDP, cyclic bifunctional) and 1,1-bis(tert-butylperoxy)cyclohexane (L331, linear bifunctional). The model very adequately predicts polymerization rates and complete molecular weight distributions. The model is used to theoretically evaluate the influence of initiator structure and functionality as well as reaction conditions.

Keywords: polystyrene, multifunctional initiators, kinetics, mathematical model

***Corresponding authors:** G. Morales, Centro de Investigación en Química Aplicada (CIQA), Bv. E. Reyna Hermosillo 140, C.P. 25294, Saltillo, Coahuila, México, E-mail: graciela.morales@ciqa.edu.mx
D. Estenoz, Department of Chemical Engineering, Instituto Tecnológico de Buenos Aires (ITBA), Av. Madero 399, C.P.1106, Buenos Aires, Argentina; Instituto de Desarrollo Tecnológico para la Industria Química, INTEC (Universidad Nacional del Litoral – CONICET), Güemes 3450, C.P. 3000, Santa Fe, Argentina, E-mail: destenoz@santafe-conicet.gov.ar
E. Berkenwald, M. L. Laganá, Department of Chemical Engineering, Instituto Tecnológico de Buenos Aires (ITBA), Av. Madero 399, C.P.1106, Buenos Aires, Argentina
P. Acuña, Centro de Investigación en Química Aplicada (CIQA), Bv. E. Reyna Hermosillo 140, C.P. 25294, Saltillo, Coahuila, México

1 Introduction

Polystyrene (PS) is a widely used thermoplastic, mainly produced by a bulk process involving the free-radical polymerization of styrene (St) in the presence of a chemical initiator (Scheirs and Priddy 2003).

A typical monofunctional initiator for a free-radical polymerization process contains one labile group (e.g. peroxide group), which generates radicals upon decomposition, chemically initiating the polymerization reaction. With this type of initiator, it has been proven difficult to achieve an appropriate balance between residence times, polymerization rates, molecular weights and polydispersities, while also maintaining high conversions – the latter in order to maximize process productivity and minimize residual monomer concentration in the product (Yoon and Choi 1992; Gonzalez, Meira, and Oliva 1996; Scheirs and Priddy 2003). In recent decades, the use of multifunctional initiators (i.e. molecules containing more than one radical-generating labile group) provided a solution to the former problem. This type of initiator allows obtaining both high reaction rates and molecular weights, while also enhancing final properties of the product (Choi and Lei 1987; Kim and Choi 1989; Villalobos, Hamielec, and Wood 1991; Estenoz et al. 1996; Cavin et al. 2000). This improvement was attributed to the existence of additional radical-generating reactions given by the rupture of undecomposed labile groups, which are disseminated in the growing and temporarily dead polymer chains. These species can be involved in further initiation, propagation, chain transfer and termination reactions during the course of polymerization, leading to high average molecular weights. This behavior is usually attributed to the sequential rupture of the initiator molecule (Kim and Choi 1989). This and other works have theoretically studied the synthesis of PS with bifunctional initiators and developed mathematical models to predict the reacting species concentrations and the molecular structure of the obtained polymer in the course of the polymerization reaction. Kuchanov, Ivanova, and Ivanchev (1976) studied different mono-, bi-, and trifunctional peroxide-type initiators of similar structures at a

constant peroxide concentration and found similar polymerization rates that were independent of the initiator employed, provided the peroxide groups have a similar thermal stability. In Ivanov, Kuchanov, and Ivanchev (1977), a statistical model was proposed for polymerization using multifunctional initiators. A few years later, Choi and Lei (1987) and Kim and Choi (1989) developed detailed kinetic models for the bulk styrene homopolymerization with symmetrical and asymmetrical diperoxyster initiators. They showed that at high temperatures, it is possible to obtain both high reaction rates and molecular weights with relatively narrow molecular weight distributions (MWDs). Villalobos, Hamielec, and Wood (1991) theoretically and experimentally investigated the polymerization of St with bifunctional initiators 2,5-di-methyl-2,5-bis(2-ethylhexanol peroxy) hexane (Lupersol-256, L-256), 1,1-di(t-butyl peroxy) cyclohexane (Lupersol-331-80B), and 1,4-bis(t-butyl peroxy) cyclohexane (D-162). Compared to the standard monofunctional case, bifunctional initiators exhibited a reduction in polymerization time of up to 75% without substantial changes in the final product properties. Both considerably high reaction rates and molecular weights were observed.

The majority of experimental and modeling works involved bifunctional initiators, specifically in the polymerization of St. Works involving experimental studies and modeling of polymerization systems using initiators with functionalities greater than two in free radical polymerization are less numerous (Cerna et al. 2002; Scolah, Dhib, and Penlidis 2006; Galhardo, Magalhães Bonassi Machado, and Ferrareso Lona 2012; Sheng et al. 2004). Cerna et al. (2002) experimentally studied the bulk polymerization of styrene using initiators with different functionalities (monofunctional, bifunctional, and trifunctional initiators). In Scolah, Dhib, and Penlidis (2006), the bulk polymerization of St and methyl methacrylate in the presence of the tetrafunctional initiator polyether poly(t-butyl peroxy carbonate) (JWEB50) was experimentally and theoretically studied. The developed model allowed the calculation of global variables such as monomer conversion, average molecular weights, and average polymer structure; and was validated with experimental results. Works comparing monofunctional with bifunctional initiators can also be found in the literature (Gonzalez, Meira, and Oliva 1996; Yoon and Choi 1992; Choi and Lei 1987; Kim and Choi 1989; Cavin et al. 2000) as well as works employing mixtures of mono- and bifunctional initiators (Gonzalez, Meira, and Oliva 1996).

With respect to initiator structure, it was observed that the use of cyclic multifunctional initiators (e.g.: triperoxide

cyclohexanone (CHTP), diethylketone triperoxide (DEKTP), acetone triperoxide (ATP), cyclohexanone diperoxide (CHDP) and pinacolone diperoxide (PDP)) in polymerization reactions represents a promising alternative (Sheng et al. 2004; Castañeda Facio 2007; Berkenwald et al. 2013; Berkenwald et al. 2015). Sheng et al. (2004) experimentally studied the use of the cyclic trifunctional initiator 3,6,9-triethyl-3,6,9-trimethyl-1,4,7-triperoxonane in the bulk polymerization of St. The results also showed that it is possible to produce polymers with higher molecular weights and lower polydispersities at a higher rate. The obtained PS had remaining “O-O” bonds in the molecular chains. In Berkenwald et al. (2013), the use of diethyl ketone triperoxide (DEKTP), a cyclic trifunctional peroxide initiator, in the bulk polymerization of St was experimentally and theoretically studied. A mathematical model was developed to predict the evolution of the reacting species concentration, monomer conversion, and detailed polymer molecular structure. In this study, initiation by DEKTP at 120–130°C yielded polymers with high molecular weights, depending on the DEKTP concentration at relatively short polymerization times. The authors also studied the bulk polymerization of styrene using DEKTP at higher temperatures (150–200°C) (Berkenwald et al. 2015). Experimental and theoretical results are consistent with a total rupture of the initiator molecule at these higher temperatures, resulting in lower average molecular weights. The working temperature zone of technological interest for the use of a multifunctional initiator is therefore that where initiator decomposition is mostly sequential.

With respect to the theoretical determination of the detailed molecular structure of PS obtained in the bulk polymerization of St using multifunctional initiators, relatively few works are available in the literature, due to complexity of the polymerization system and the high calculation times involved in detailed species distributions. When considering cyclic multifunctional initiators, multi-radical species may be generated and the polymer species will have undecomposed peroxide groups within their chains. Their position inside the chain should be estimated in order to evaluate the effect of the re-initiation reactions on the molecular weight distribution. Mathematical models based on moment equations can adequately predict the obtained average molecular weights, but fail to evaluate the full molecular weight distribution (MWD) (Scolah, Dhib, and Penlidis 2006). If the mathematical models were used for simulating the complete industrial polymerization process, it is of importance that the detailed polymer MWD be simulated due to its effect on quality variables such as oligomer content, mechanical properties and processing properties

(Seavey et al. 2003). In addition, the mathematical models involving multifunctional initiators are limited to specific cases, in terms of initiator functionality and structure (Gonzalez, Meira, and Oliva 1996; Yoon and Choi 1992; Choi and Lei 1987; Kim and Choi 1989; Cavin et al. 2000; Sheng et al. 2004; Scolah, Dhib, and Penlidis 2006; Berkenwald et al. 2013; Berkenwald et al. 2015). These models cannot be readily applied to initiators with other functionalities or structures, where more complex kinetics may be involved.

This work is the first attempt to develop a comprehensive mathematical model for a bulk styrene polymerization system initiated by multifunctional initiators. An advantageous feature of this model is that it allows the estimation of the evolution of the detailed MWD of each polymer species, and full information about the molecular structure of the obtained product. Additionally, this model is a comprehensive model, in the sense that it can be used to simulate any mono- or multifunctional initiator, either linear or cyclic. The model was adjusted and validated using new experimental results for the bulk polymerization of St using different peroxide initiators in a batch reactor. The model is then used to theoretically study the use of multifunctional initiators and the effect of process conditions on polymerization rate and product quality.

2 Experimental work

The experimental work consisted on the synthesis and characterization of the organic peroxide PDP and isothermal batch bulk polymerizations of St using the multifunctional initiators PDP and L331 at 0.01 mol/L. The experimental data for bulk polymerization of styrene using the trifunctional cyclic initiator DEKTP were taken from our previous work (Berkenwald et al. 2013). The selected polymerization temperatures are such that initiator decomposition is mostly sequential (Cerna et al. 2002; Casteñeda Facio 2007).

2.1 Reagents

Styrene (St, 99%) was provided by Sigma-Aldrich and it was purified by vacuum distillation over sodium before use. 1,1-Bis(tert-butylperoxy)cyclohexane (Luperox-331M80) was supplied by Arkema and it was used as received. Ammonium chloride (NH_4Cl , $\geq 99.5\%$), 3-pentanone ($\geq 99\%$), 3,3-dimethyl-2-butanone (98%), sodium sulfate anhydrous (Na_2SO_4 , $\geq 99\%$), petroleum ether (ACS

reagent), methanol (99.8%) and tetrahydrofuran (THF, $\geq 99\%$) were supplied by Sigma-Aldrich and they were used without extra purification. Sulfuric acid (H_2SO_4 , 98%) and hydrogen peroxide (H_2O_2 , 50%) were purchased from J. T. Baker and they were used as received.

2.2 Synthesis of PDP

Pinacolone diperoxide (PDP) was obtained according to a method reported in the literature (Casteñeda Facio 2007). 50 mmol of 3,3-dimethyl-2-butanone were dripped into a stirred mixture of H_2O_2 (56 mmol) and H_2SO_4 (195 mmol) at -15 to -20°C . After 3 hours of reaction, the mixture was extracted with petroleum ether (3×25 mL). The organic layer was freed of H_2O_2 by washing with a saturated solution of NH_4Cl (3×10 mL) and with water (3×10 mL). The organic layer was dried over Na_2SO_4 for 24 hours. The solution was filtered and the product was isolated by solvent evaporation. The obtained white solid was recrystallized twice from methanol and its purity was confirmed by nuclear magnetic resonance (NMR).

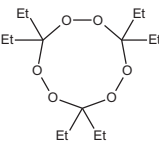
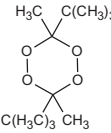
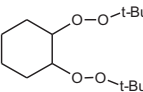
2.3 Polymerization reactions

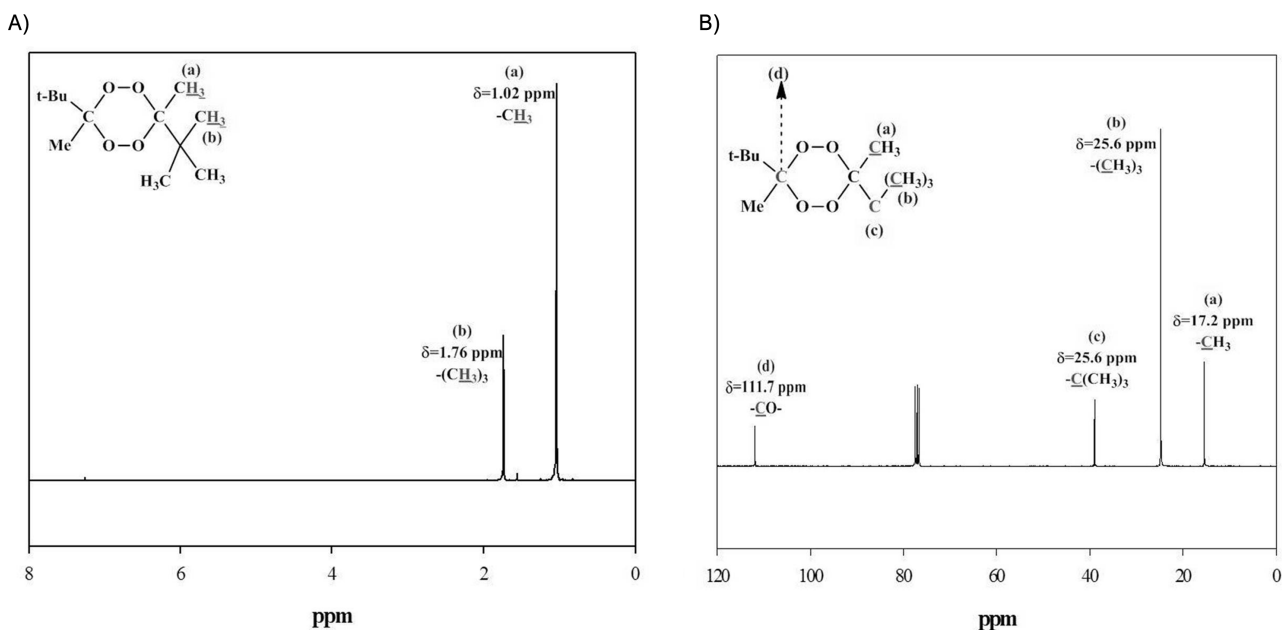
A metal polymerization reactor was filled with 900 mL of St, and initiator was added in order to reach 0.01 mol/L for all initiators. The reaction mixture was de-gassed and blanketed with nitrogen and the reactor was heated to the selected temperature with a heating coil containing flowing hot oil. The peroxide initiators employed and reaction conditions are summarized in Table 1. Note that polymerizations using DEKTP were taken from Berkenwald et al. (2013) The reaction temperature was monitored and controlled using a 4842 PID controller and an air-cooling system in order to keep the temperature at the desired value. The stirring rate was 50 rpm. Samples were taken along the reaction using a sampling valve located at the bottom of the reaction vessel. The samples were then dissolved in 10 times their volume of toluene under agitation.

2.4 Analytical techniques

Cyclic peroxide initiator PDP was characterized by ^1H and ^{13}C NMR using a JEOL Eclipse-300 MHz spectrometer. CDCl_3 was used as solvent and analyses were

Table 1: Multifunctional initiators and reaction conditions.

Initiator (0.01 mol/L)			Temperature (°C)	
Name	IUPAC Name	Initiator type	Chemical structure	
Diethyl ketone triperoxide (DEKTP)	3,3,6,6,9,9-hexaethyl-1,2,4,5,7,8-hexaoxacyclononane	Cyclic trifunctional		120 130
Pinacolone diperoxide (PDP)	3,6-ditertbutyl-3,6-dimethyl-1,2,4,5-tetraoxacyclohexane	Cyclic bifunctional		110 120
Luperox-331M80 (L331)	1,1-Bis(tert-butylperoxy)cyclohexane	Linear bifunctional		110 116

**Figure 1:** NMR Spectra for Synthesized PDP: A) ^1H NMR B) ^{13}C NMR.

performed at room temperature. The resulting NMR spectra are presented in Figure 1.

Polymers were isolated from the samples by precipitation in methanol and filtration. Conversion was determined by gravimetric analysis from the weights of the samples and the weight of the filtered, dry polymer.

Molecular weights of polymer samples were determined by size exclusion chromatography (SEC) at 40°C using a Hewlett-Packard instrument (HPLC series 1100) equipped with UV light and refractive index detectors. A series of three PLGel columns at porosities of 10^3 , 10^5 , and 10^6 Å was used. Calibration was carried out with PS

standards and THF (HPLC grade) was used as eluent at a flow rate of 1 mL/min.

2.5 Experimental results

The results for conversion and average molecular weights of the experiments of Table 1 are presented in Figure 2. Experimental results for the molecular weights distributions at the end of polymerization are presented in Figure 3.

The experimental results show that polymerizations rates are higher for PDP than for DEKTP at equivalent

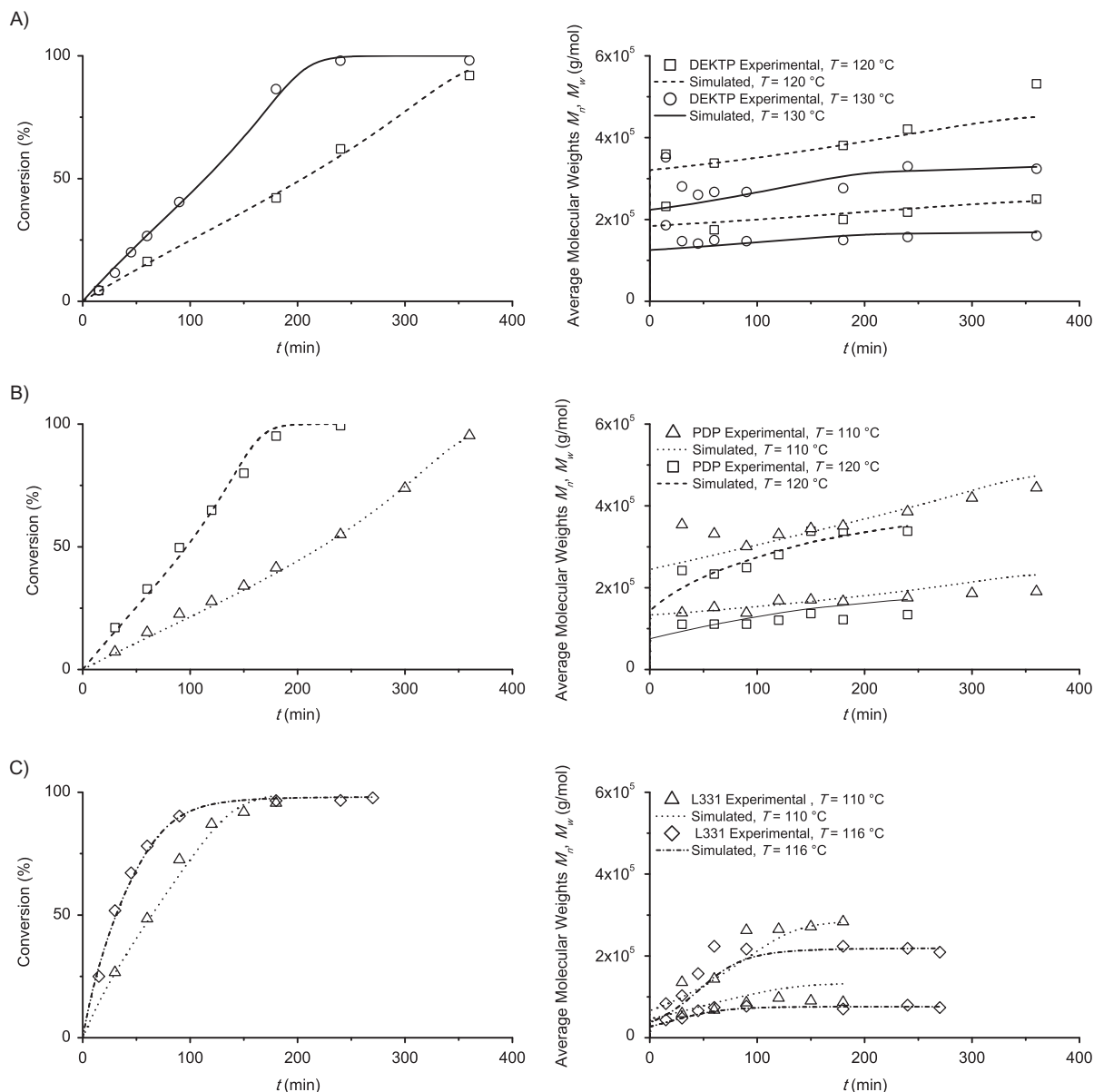


Figure 2: Conversion and Average Molecular Weights as functions of time for A) DEKTP, B) PDP and C) L331.

reaction temperature and initial initiator concentration. Further, initiation by L331 provides a higher initial polymerization rate than the one for PDP at the same temperature of 110°C . As expected, increasing the reaction temperature increases the initial polymerization rate.

It is observed that PDP initiation provides a greater initial R_p compared to DEKTP, indicating that the peroxide groups in PDP are less stable than those of DEKTP. The stability of peroxide groups inside the initiator molecules has been theoretically investigated using molecular

simulations, which have shown that several stable conformers exist for DEKTP, while only two are stable in the case of PDP (Delgado Rodríguez et al. 2014). Similarly, the peroxide groups in L331 would be less stable than those in PDP. As regards the molecular weights, it can be seen that higher molecular weights are obtained when using DEKTP with respect to PDP and L331. This can be attributed to a higher stability – and lower decomposition rate – of peroxide groups in cyclic initiators, as well as the presence of di-radicals in the reaction system.

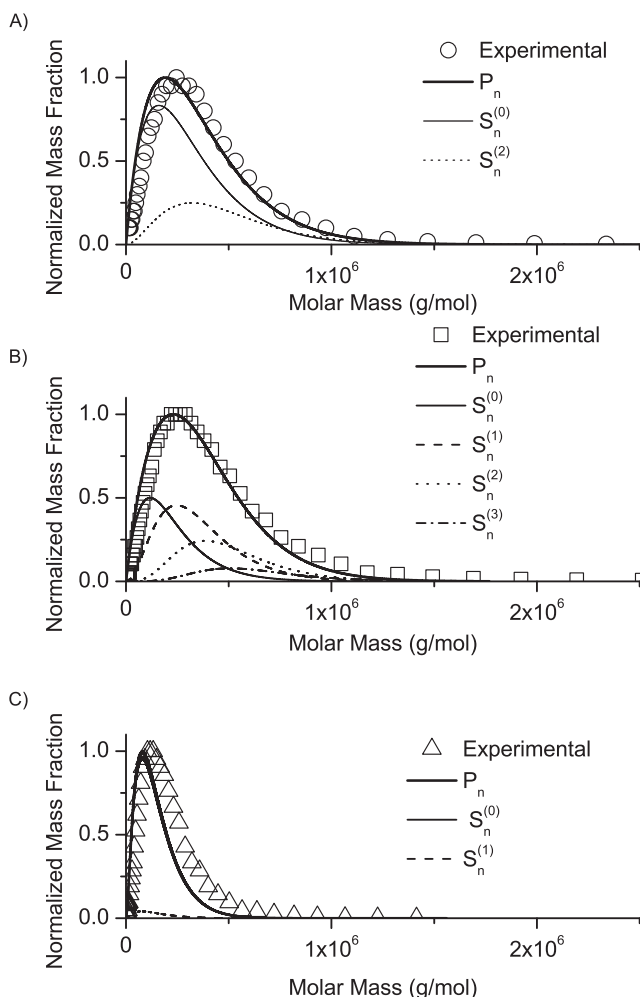


Figure 3: Experimental and theoretical MWDs for A) DEKTP, T = 130 °C, B) PDP, T = 120 °C, C) L331, T = 116 °C.

3 Mathematical model

3.1 Polymerization model

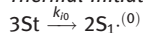
The mathematical model is based on the kinetic mechanism presented in Table 2, which includes initiation via a symmetrical cyclic or linear multifunctional initiator, thermal initiation, propagation, transfer to the monomer, combination termination and re-initiation. The following nomenclature was used:

- $I^{(\phi)}$ Cyclic multifunctional initiator with ϕ undecomposed peroxide groups.
- $\bar{I}^{(\phi)}$ Linear multifunctional initiator with ϕ undecomposed peroxide groups.
- $\cdot I \cdot^{(i)}$ Initiator diradical with i undecomposed peroxide groups.

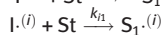
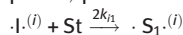
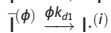
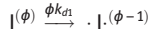
Table 2: Adopted kinetic mechanism.

Initiation ($\phi = 1, 2, 3; i < \phi$)

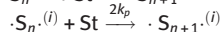
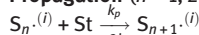
Thermal initiation



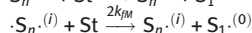
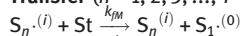
Chemical initiation



Propagation ($n = 1, 2, 3, \dots; i = 0, 1, 2, \dots$)

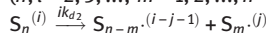


Transfer ($\eta = 1, 2, 3, \dots; i = 0, 1, 2, \dots$)

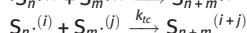
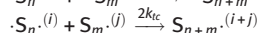
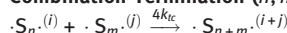


Re-initiation

($n, l = 2, 3, \dots; m = 1, 2, \dots, n-1; i = 1, 2, \dots; j = 0, 1, 2, \dots, i-1$)



Combination Termination ($n, m = 1, 2, 3, \dots; i, j = 0, 1, 2, \dots$)



- $I \cdot^{(i)}$ Initiator monoradical with i undecomposed peroxide groups.
- $\cdot S_1 \cdot^{(i)}$ Monomer diradical with i undecomposed peroxide groups.
- $S_1 \cdot^{(i)}$ Monomer monoradical with i undecomposed peroxide groups.
- $S_n \cdot^{(i)}$ PS monoradical of chain length n containing i undecomposed peroxide groups.
- $\cdot S_n \cdot^{(i)}$ PS diradical of chain length n containing i undecomposed peroxide groups.
- $S_n \cdot^{(i)}$ Polymer with n repetitive units of St and i undecomposed peroxide groups.

The following was considered: (i) at the temperatures employed, the initiator decomposition was due exclusively to sequential decomposition (Villalobos, Hamielec, and Wood 1991; Cerna et al. 2002; Castañeda Facio 2007); (ii) intra-molecular termination is negligible (Estenoz et al. 1996); (iii) disproportion termination is negligible (Duerksen and Hamielec 2007); (iv) all peroxide groups present in the initiator and in the accumulated polymer exhibited the same thermal stability Estenoz et al. 1996); (v) because of the short lifetime of radicals, the decomposition of undecomposed peroxide groups does not occur in radical molecules (Estenoz et al. 1996); (vi) propagation and transfer reactions are unaffected by the chain length or conversion (Estenoz et al. 1996); (vii) degradation reactions are negligible (Hui and Hamielec 1972).

Note the following:

(1) when two mono-radicals with i and j undecomposed peroxide groups terminate, the formed polymer will contain $i + j$ undecomposed peroxide groups; (2) with a cyclic trifunctional initiator, di-radicals only have an even number of peroxide groups, as they are generated only by propagation of the initiator di-radical (with only two peroxide groups) and by the combination termination of other di-radicals, all of which have an even number of peroxide groups; (3) re-initiation involves the decomposition of a peroxide group within a polymer chain with undecomposed peroxide groups, which generates two mono-radicals capable of further growth. Because of the molecular structure of the initiator molecules considered, only linear di-radicals and mono-radicals and linear polymer chains can be formed in the reaction system.

At temperatures of 110–130°C, peroxide groups in the initiators considered in this work decompose sequentially, and thus polymeric species containing undecomposed peroxide groups are generated. Said species can further decompose during the course of polymerization, adding to the complexity of the polymerization mechanism. Both the radical and polymer chain length distributions are modified by the rupture of one of these peroxide groups. Even though the values for the average molecular weights could be obtained by a moments-based mathematical model, a more detailed model is required in order to simulate the evolution of the full MWD.

A first-order, bi-dimensional, non-linear polymerization model was developed from the kinetic mechanism detailed in Table 2. The model consists of a set of non-linear differential equations, which are derived from the mass balances for the reacting species (see Appendix), including the living radical species, dead and temporarily dead polymer species for all kinetic chain lengths and number of undecomposed peroxide groups.

The mathematical model consists of three modules:

- The Basic Module (Appendix A), which allows the prediction of global chemical species evolution along the reaction (total mono-radicals and di-radicals, total polymer).
- The Moments Module (Appendix B), consisting of equations for the evolution of the 0th, 1st and 2nd moments of the reacting species chain length distributions. Said moments can be used to estimate the evolution of average molecular weights during the course of polymerization.
- The Distributions Module (Appendix C), which simulates the evolution of all chemical species, characterized by their chain length and number of undecomposed peroxide groups. The equations

estimate the evolution of the complete MWD of each radical and polymer species. In order to consider the effect of re-initiation reactions in the MWDs, polymer chains were assumed to have uniformly distributed peroxide groups. A random-chain scission can be simulated with a uniformly distributed random variable. The uniform peroxide group distribution hypothesis is expected to be valid for cyclic initiators and for linear initiators with functionalities greater than two.

The proposed model considers an ideal cooling/heating system, which allows the polymerization temperature to be set at a specific value. However, the effect of temperature on reaction kinetics is considered through the use of Arrhenius expressions for the kinetic parameters. The gel effect was indirectly considered by appropriately reducing the value of the termination kinetic coefficient with increasing conversion (Hui and Hamielec 1972)

The Basic Module can be solved independently from the other two, and for its resolution, eqs (1)–(4), (7), (8), and (20)–(22) must be simultaneously solved. For predicting polymer molecular structure, the Moments Module or alternatively the Distributions Modules can be solved using the results from the Basic Module, in order to estimate the average molecular weights or the detailed MWD of the polymer species, respectively.

The Basic and Moments modules are solved by standard stiff differential equation numerical methods based on a second-order modified Rosenbrock formula, programmed in MATLAB v. 8.3. In the Distributions Module, a large number of equations (>500,000) must be integrated. For this reason, an explicit forward Euler method was used, with the time intervals obtained from resolution of the basic module. A typical simulation requires less than 1 s for the Basic Module, 1 min for the Moments Module and about 5 min for the distribution module with an Intel Core i5 based processor at 2.40 GHz. These calculation times are considerably shorter than what is reported with similar moments-based models for multifunctional initiators (Maafa, Soares, and Elkamel 2007).

3.2 Simulation results

The model was adjusted using the experimental data in Figures 2 and 3. Model parameter adjustment was sequential and consisted of two steps, using least-squares optimization algorithms. Firstly, k_{d1} , k_{dp} , f_1 and f_2 for each initiator were adjusted with the conversion data. Since all peroxide groups are assumed to have the thermal stability, $k_{dp} = k_{d1}$ and it was assumed that

$f_1 = f_2$. Secondly, k_{fM} was adjusted with the average molecular weight data. The obtained values for the decomposition constants are in accordance with what has been reported for the decomposition rates of organic peroxides (Cerna et al. 2002), and the values for the transfer constants are within the expected range reported in the literature (Meyer and Keurentjes 2005). All other values for the kinetic parameters were taken from the literature (Hui and Hamielec 1972). Model parameters are presented in Table 3.

Model parameter adjustment yields k_{d1} (L331) $<$ k_{d1} (PDP) $<$ k_{d1} (DEKTP), their differences being of orders of magnitude, which is in agreement with the experimental results. The higher value for L331 is related to the higher initial R_p , as discussed earlier. In addition, simulation results indicate that, in the case of L331 at 116°C, the initiator is totally consumed at around 100 min, which is in agreement with the experimental results, as the slope of the conversion curve decreases at around 100 min at 116°C. Once the initiator is fully consumed, the system becomes almost exclusively thermally activated and the R_p decreases.

As it can be observed in Figures 2 and 3, theoretical and experimental results are in very good agreement. The differences in molecular weights are, in all cases, within the experimental error range (below 10%). Note that the major differences in molecular weight values occur for the linear bifunctional initiator L331. The result is expected due to the uniform peroxide group distribution hypothesis. As an additional verification, simulations were carried out modifying the peroxide group distribution for the specific case of a

bifunctional linear initiator, for which all peroxide groups are located at chain ends (see Appendix C). In this case, as expected, a broader simulated molecular weight distribution is obtained, which is in better agreement with the experimental values.

To confirm the consistency of the different modules, the following verifications were carried out:

- It was verified that the results from the Basic, Moments and Distributions Modules were equivalent. Specifically, it was verified that average molecular weights calculated with the Moments Module had the same values as the MWD averages obtained with the Distributions Modules, conversion calculated with Distributions Module matched the one calculated with the Basic Module and that peroxide group concentrations calculated by the Basic, Moments and Distributions Modules are equivalent.
- It was verified that, when using the initiator L331 (linear bifunctional), polymers had a maximum of two undecomposed peroxide groups. This is because with a bifunctional linear initiator, polymer species with more than two peroxide groups are not generated in the course of polymerization.

Other simulation results using the model are presented in Figure 3, Figure 4 and Table 4.

Figure 4 shows the evolution of the total polymer species concentrations as functions of conversion, characterized by the number of (undecomposed) peroxide groups, as defined by eq. (44). The simulated conditions correspond to the conditions in Table 1.

Table 3: Kinetic parameters.

Kinetic parameter	Units	Arrhenius expression	References
k_{d1}, k_{dp} (DEKTP)	$[s^{-1}]$	$4.0e^{-5440/T}$	Adjusted in this work
k_{d1}, k_{dp} (PDP)	$[s^{-1}]$	$7.0 \cdot 10^{17}e^{-19761/T}$	Adjusted in this work
k_{d1}, k_{dp} (L331)	$[s^{-1}]$	$5.0 \cdot 10^{20}e^{-21331/T}$	Adjusted in this work
f_1, f_2 (DEKTP)		$0.03T - 11.29$	Adjusted in this work
f_1, f_2 (PDP)		$0.0025T - 0.708$	Adjusted in this work
f_1, f_2 (L331)		$0.0033T - 12.32$	Adjusted in this work
k_{i0}	$\left[\frac{L^2}{mol^2 s} \right]$	$2.19 \cdot 10^5 e^{-13810/T}$	Hui and Hamielec (1972)
k_{i1}, k_p	$\left[\frac{L}{mol s} \right]$	$1.051 \cdot 10^7 e^{-3557/T}$	Hui and Hamielec (1972)
k_{fM}	$\left[\frac{L}{mol s} \right]$	$7.0 \cdot 10^{10} e^{-10185/T}$	Adjusted in this work
k_{tc}	$\left[\frac{L}{mol s} \right]$	$1.686 \cdot 10^9 e^{-(844/T) - 2(C_1x + C_2x^2 + C_3x^3)^a}$	Hui and Hamielec (1972)

Note: $^a C_1 = 2.57 - 0.00505T$; $C_2 = 9.56 - 0.0176T$; $C_3 = -3.03 + 0.00785T$, with x monomer conversion.

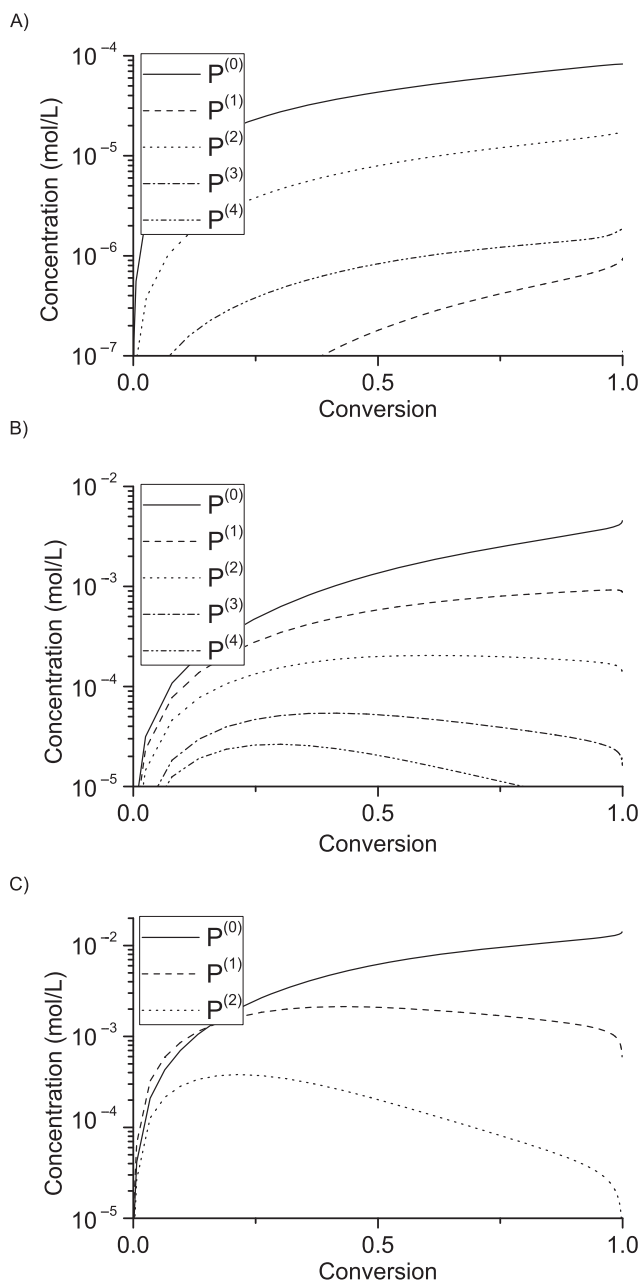


Figure 4: Evolution of the Polymeric Species for A) DEKTP, $T=130\text{ }^{\circ}\text{C}$, B) PDP, $T=120\text{ }^{\circ}\text{C}$, C) L331, $T=116\text{ }^{\circ}\text{C}$.

Table 4: Theoretical study of initiator functionality and structure in a St polymerization process.

Functionality	Structure	$\bar{R}_p, 100\% \times 10^4$ ($\text{mol} \cdot \text{L}^{-1} \cdot \text{s}^{-1}$)	$\bar{M}_n \times 10^{-5}$ (g/mol)	$\bar{M}_w \times 10^{-5}$ (g/mol)
3	Cyclic	3.19	2.80	5.31
3	Linear	3.20	2.15	3.95
2	Cyclic	3.19	2.77	5.20
2	Linear	3.20	2.12	3.96
1	Cyclic	3.19	2.73	5.37
1	Linear	3.19	2.09	4.01

In Figure 4, it can be observed that species containing different numbers of peroxide groups are generated in the polymerization system. For these systems, the polymer without peroxide groups is the most abundant polymer species. These species is mainly generated by thermal initiation of the monomer.

In the case of the trifunctional cyclic initiator DEKTP and $130\text{ }^{\circ}\text{C}$, the species with two peroxide groups is the most abundant peroxide-containing species. This is because said polymer species is generated mostly by chemical initiation, and the propagation initiator di-radical contains two peroxide groups. The polymer with one peroxide group is generated at around 10% conversion, since the polymer with two peroxide groups must decompose in order to generate a growing chain containing one peroxide group. An analogous reasoning applies to polymers with a higher number of peroxide groups. It should be noted that polymers with an even number of peroxide groups are also generated by termination between two initiator di-radicals and further propagation of the generated di-radical (containing an even number of peroxide groups), accounting for their higher concentrations in the system. For the peroxide-containing species, the speed of generation exceeds that of decomposition, and their concentration increases with conversion.

In the case of the bifunctional cyclic initiator PDP at $120\text{ }^{\circ}\text{C}$, initiator decomposition generates a growing di-radical with one undecomposed peroxide group. As the decomposition rate is higher than for the case of DEKTP, and the contribution of thermal initiation is lower, a larger number of peroxide containing species is generated. In the case of the species with a high number of peroxide groups (three or four), the rate of decomposition can exceed the rate of generation, and the polymer concentration can decrease with increasing conversion. Before the system reaches full conversion, the polymer with three peroxide groups is almost fully consumed and the polymer with four peroxide groups is fully consumed.

In the case of the linear bifunctional initiator L331 at $116\text{ }^{\circ}\text{C}$, the decomposition rate is highest, and the contribution of thermal initiation is lowest. The polymer containing one peroxide group, generated by propagation of the initiator radical, is in a larger proportion than the polymer without peroxide groups at very early stages in the polymerization. However, due to the decomposition of the peroxide groups, its concentration eventually decreases. The polymer with two peroxide groups is fully consumed before the system reaches full conversion. Due to the linear structure of the initiator molecule,

polymers with a higher number of peroxide groups are not generated in this system.

In Figure 3, the MWDs of the most relevant molecular species, characterized both by chain length and number of peroxide groups, are presented. As expected, the polymer without peroxide groups is the most abundant species at the end of the polymerization for all initiators. As previously stated, in the case of DEKTP the polymer with two peroxide groups is the most abundant among these peroxide-containing species. In the case of PDP, due to the lower temperature and lower decomposition rate of the peroxides, a greater number of polymer species containing peroxide groups is present at the end of the polymerization. The polymer with one peroxide group, mainly generated from an initiator radical, is the most abundant peroxide-containing polymer species. In the case of L331, only a small fraction of polymer with one peroxide group remains in the system at the end of polymerization, due to the very high decomposition rate of the peroxide groups.

The model was also used to theoretically evaluate the influence of initiator functionality and structure in different polymerization processes. A series of simulations were carried out, corresponding to theoretical experiments, varying the initiator functionality and structure for given process conditions. In all of the simulations, it was assumed that the peroxide groups have a decomposition constant of $k_{dt} = k_{dp} = 4 \times 10^{-6} \text{ s}^{-1}$ and $f_1 = f_2 = 0.5$ at a temperature of 120°C . For the simulations, the functionality and structure of the initiators were varied, while the initial peroxide group concentration was set to 0.02 mol/L for all simulated initiators, so that the results can be compared. Simulation results are presented in Table 4.

As expected, all initiators provide equivalent rates of polymerization, if the same initial peroxide group concentration is used. The fact that the rate of initiation is independent of initiator functionality when all peroxides have the same thermal stability was already experimentally verified in the work of Kuchanov, Ivanova, and Ivanchev (1976). It is also observed that higher average molecular weights are obtained when using initiators with higher functionalities, as the effect of re-initiation reactions on molecular weights is increased. A cyclic initiator provides higher average molecular weights than a linear one of the same functionality. This is explained by the fact that di-radicals can propagate by their two ends, generating longer chain radicals. In addition, termination or transfer reactions of di-radicals can form monoradicals, capable of further

propagation and growth. The effect on polymerization rate of the di-radicals containing two active reacting sites is small, since the concentration of monoradicals exceeds that of di-radicals, due to thermal decomposition.

If a hypothetical family of initiators were to be synthesized, for which all peroxide groups had the same thermal stability, theoretical results show that:

- A cyclic initiator provides higher average molecular weights compared with a corresponding linear one, by about 30%. The structure of the initiator has little effect on the rate of polymerization.
- At the same initiator concentration, an initiator of higher functionality provides higher polymerization rates and higher average molecular weights.
- At the same initial peroxide group concentration, an initiator of higher functionality provides higher average molecular weights while maintaining a high polymerization rate.

4 Conclusions

A comprehensive mathematical model was presented, which simulates the evolution of all the chemical species in the course of a bulk polymerization of styrene using multifunctional initiators in a batch reactor. The model was adjusted and validated using the experimental data from batch reactions using initiators DEKTP, PDP and L331. The proposed kinetic mechanism considers the re-initiation reactions due to undecomposed peroxide groups within the polymer chains, and the derived model can be used to evaluate the molecular structure of the obtained polymer. Theoretical and experimental results indicate that initiator structure and functionality are key variables determining initiator performance. An initiator of a high functionality and a cyclic structure provides polymers of high molecular weights, while maintaining high polymerization rates.

The model can be used to simulate an industrial process with a polymerization initiator of a specific functionality and structure and for plant optimization purposes. The model can be extended to a continuous process and adapted for initiator mixtures.

Funding: Consejo Nacional de Investigaciones Científicas y Técnicas (Grant/Award Number: “PICT 2011-1254”).

Appendix A: Basic module

Balances for the non-polymeric reagents and products

Multifunctional Initiators ($\phi = 1, 2, 3$)

$$\frac{d}{dt} \left([I^{(\phi)}] V \right) = -\phi k_{d1} [I^{(\phi)}] V \quad (1)$$

$$\frac{d}{dt} \left([\bar{I}^{(\phi)}] V \right) = -\phi k_{d1} [\bar{I}^{(\phi)}] V \quad (2)$$

Secondary Initiator Species ($\phi > i = 1, 2$)

$$\frac{d}{dt} \left([I^{(i)}] V \right) = -i k_{d1} [I^{(i)}] V + (1 - f_1) \sum_{j=i+1}^{\phi} j k_{d1} \left([I^{(j)}] + [\bar{I}^{(j)}] \right) V \quad (3)$$

Monomer

Assuming the “long chain approximation” (by which propagation is the only monomer-consuming reaction):

$$\frac{d}{dt} ([St] V) = -R_p V = -k_p [St] ([R\cdot] + 2[R\cdot\cdot]) V \quad (4)$$

where R_p is the global St polymerization rate, and

$$[R\cdot] = \sum_{i=0}^{\infty} \sum_{n=1}^{\infty} [S_n^{(i)}] \quad (5)$$

$$[R\cdot\cdot] = \sum_{i=0}^{\infty} \sum_{n=1}^{\infty} [\bar{S}_n^{(i)}] \quad (6)$$

represent the total concentrations of mono- and diradicals respectively.

Radical species ($i = 0, 1, \dots, n = 2, 3, \dots$)

Consider the mass balances of all free radical appearing in the global kinetics. Such balances provide:

$$\frac{d}{dt} \left([I^{(i)}] V \right) = f_1 (i+1) k_{d1} [I^{(i+1)}] V - 2k_{i1} [St] [I^{(i)}] V \quad (7)$$

$$\frac{d}{dt} \left([I^{(i)}] V \right) = \sum_{j=i+1}^{\phi} p_j(i) f_j j k_{d1} [\bar{I}^{(j)}] V - k_{i1} [St] [I^{(i)}] V \quad (8)$$

Where $p_i(j)$ is the probability that the decomposition of the initiator of functionality j generates a monoradical with i undecomposed peroxide groups.

$$\frac{d}{dt} \left([S_1^{(i)}] V \right) = 2k_{i1} [I^{(i)}] [St] V - 2(k_p [St] + k_{fM} [St] + k_{tc} ([R\cdot] + 2[R\cdot\cdot])) [S_1^{(i)}] V \quad (9)$$

$$\begin{aligned} \frac{d}{dt} \left([S_n^{(i)}] V \right) &= 2k_p [St] \left([S_{n-1}^{(i)}] - [S_n^{(i)}] \right) V \\ &\quad - 2(k_{fM} [St] + k_{tc} ([R\cdot] + 2[R\cdot\cdot])) [S_n^{(i)}] V \\ &\quad + 2k_{tc} \sum_{j=0}^i \sum_{m=1}^{n-1} [S_{n-m}^{(i-j)}] [S_m^{(j)}] V \end{aligned} \quad (10)$$

$$\begin{aligned} \frac{d}{dt} \left([S_1^{(i)}] V \right) &= \left\{ k_{i1} [I^{(i)}] [St] + \delta_{i0} \left(2k_{i0} [St]^3 \right. \right. \\ &\quad \left. \left. + k_{fM} [St] ([R\cdot] + 2[R\cdot\cdot]) \right) \right\} V \\ &\quad - (k_p [St] + k_{fM} [St] + k_{tc} ([R\cdot] + 2[R\cdot\cdot])) [S_1^{(i)}] V \end{aligned} \quad (11)$$

Where δ_{i0} is the Kronecker Delta ($\delta_{i0} = 1$ if $i = 0$ and $\delta_{i0} = 0$ otherwise).

$$\begin{aligned} \frac{d}{dt} \left([S_n^{(i)}] V \right) &= \left(k_p \left([S_{n-1}^{(i)}] - [S_n^{(i)}] \right) + 2k_{fM} [S_n^{(i)}] \right) [St] V \\ &\quad - \left(k_{fM} [St] + k_{tc} ([R\cdot] + 2[R\cdot\cdot]) \right) [S_n^{(i)}] V \\ &\quad + 2k_{tc} \sum_{j=0}^i \sum_{m=1}^{n-1} [S_{n-m}^{(i-j)}] [S_m^{(j)}] V \\ &\quad + f_2 k_{dp} \sum_{j=i+1}^{\infty} \sum_{m=n+1}^{\infty} \left(p_{mj}(n, i) j [S_m^{(j)}] \right) V \end{aligned} \quad (12)$$

In eq. (12), $p_{mj}(n, i)$ is the probability that a scission of a chain of dead polymer of length m and i peroxide groups yields a growing monoradical of chain length n with i peroxide groups.

Adding this probability over all i s and n s, the following can be proved:

$$\sum_{i=1}^{\infty} \sum_{n=1}^{\infty} \sum_{j=i+1}^{\infty} \sum_{m=n+1}^{\infty} p_{mj}(n, i) j [S_m^{(j)}] = \sum_{i=1}^{\infty} \sum_{n=1}^{\infty} 2i [S_n^{(i)}] = 2[Pe_{PS}] \quad (13)$$

where $[Pe_{PS}]$ is the concentration of peroxide groups in the PS chains. Note that the scission of any PS chain with undecomposed peroxide groups produces 2 monoradicals.

From eqs (9) and (10), the total concentration of diradicals may be obtained:

$$\frac{d}{dt}([\cdot R\cdot]V) = 2k_{i1} \sum_{j=0}^{\phi-1} [I^{(j)}] [St]V + 2k_{tc}[\cdot R\cdot]^2V - 2(k_{fM}[St] + k_{tc}([R\cdot] + 2[\cdot R\cdot]))[\cdot R\cdot]V \quad (14)$$

From eqs (11) and (12) and considering eq. (13), the total concentration of monoradicals may be obtained:

$$\frac{d}{dt}([R\cdot]V) = k_{i1} \sum_{j=0}^{\phi-1} [I^{(j)}] [St]V + 4k_{fM}[\cdot R\cdot][St]V + 2k_i[St]^3V - k_{tc}([R\cdot] + 2[\cdot R\cdot])[R\cdot]V + 2f_2k_{dp}[PePS]V \quad (15)$$

The total radicals are calculated as $[R\cdot] + 2[\cdot R\cdot]$. Using eqs (14) and (15),

$$\frac{d}{dt}(([\cdot R\cdot] + 2[R\cdot])V) = k_{i1} \sum_{j=0}^{\phi-1} (4[I^{(j)}] + [I^{(j)}]) [St]V + 2k_i[St]^3V + 2f_2k_{dp}[PePS]V - k_{tc}([\cdot R\cdot] + 2[R\cdot])^2V \quad (16)$$

Peroxide groups

The total concentration of peroxide groups is

$$[Pe] = \sum_{j=1}^{\phi} j ([I^{(j)}] + [\bar{I}^{(j)}]) + [PePS] \quad (17)$$

with

$$[PePS] = \sum_{i=0}^{\infty} \sum_{n=1}^{\infty} i [S_n^{(i)}] \quad (18)$$

Peroxide groups are consumed only by decomposition reactions. Therefore, it can be written

$$\frac{d}{dt}([Pe]V) = - \sum_{i=1}^{\phi} j k_{d1} ([I^{(j)}] + [\bar{I}^{(j)}])V - k_{dp}[PePS]V \quad (19)$$

Using this result and eq. (29), the molar concentration of undecomposed peroxide groups accumulated in the polymer can be calculated from the difference

$$\frac{d}{dt}([PePS]V) = \frac{d}{dt}([Pe]V) - \sum_{j=1}^{\phi} j \frac{d}{dt}([I^{(j)}] + [\bar{I}^{(j)}])V \quad (20)$$

Conversion and volume

Monomer conversion can be calculated from

$$x = \frac{[St]^0V^0 - [St]V}{[St]^0V^0} \quad (21)$$

where the superscript “0” indicates initial conditions.

The evolution of the reaction volume V is obtained from

$$V = V_{St}^0(1 - \varepsilon x) \quad (22)$$

with

$$\varepsilon = \frac{V_{St}^0 - V_S^f}{V_{St}^0} \quad (23)$$

Where V_{St}^0 is the initial St volume, ε is the St volume contraction factor and V_S^f is the final volume at full conversion.

Equations (1)–(4), (7), (8), and (20) to (22) are solved simultaneously to find the evolution of species $[I^{(i)}]$, $[\bar{I}^{(i)}]$, $[St]$, $[I^{(i)}]$, $[I^{(i)}]$, $([R\cdot] + 2[\cdot R\cdot])$, $[PePS]$, x and V .

Appendix B: Moments module

Distribution moments equations

Define the k th moment of the distribution of diradicals ($\sigma_k^{(i)}$), monoradicals ($\lambda_k^{(i)}$) and polymer ($\mu_k^{(i)}$) species, characterized by their number of undecomposed peroxide groups i :

$$\sigma_k^{(i)} = \sum_{n=1}^{\infty} n^k [S_n^{(i)}] \quad (24)$$

$$\lambda_k^{(i)} = \sum_{n=1}^{\infty} n^k [S_n^{(i)}] \quad (25)$$

$$\mu_k^{(i)} = \sum_{n=1}^{\infty} n^k [S_n^{(i)}] \quad (26)$$

The evolution of the 0th, 1st and 2nd moments of the distributions of diradicals, monoradicals and polymer species are written:

$$\frac{d(\sigma_0^{(i)}V)}{dt} = 2k_{i1} [I^{(i)}] [St]V + 2k_{tc} \sum_{j=0}^i \sigma_0^{(i-j)} \sigma_0^{(j)}V - 2 \left(k_{fM}[St] + k_{tc} \sum_{i=0}^{\infty} (\lambda_0^{(i)} + 2\sigma_0^{(i)}) \right) \sigma_0^{(i)}V \quad (27)$$

$$\begin{aligned} \frac{d(\sigma_1^{(i)} V)}{dt} &= 2k_{i1} [\cdot I \cdot^{(i)}] [\text{St}] V + 2k_p [\text{St}] \sigma_0^{(i)} V \\ &\quad + 2k_{tc} \sum_{j=0}^i (\sigma_0^{(i-j)} \sigma_1^{(j)} + \sigma_1^{(i-j)} \sigma_0^{(j)}) V \\ &\quad - 2 \left(k_{fM} [\text{St}] + k_{tc} \sum_{i=0}^{\infty} (\lambda_0^{(i)} + 2\sigma_0^{(i)}) \right) \sigma_1^{(i)} V \end{aligned} \quad (28)$$

$$\begin{aligned} \frac{d(\sigma_2^{(i)} V)}{dt} &= 2k_{i1} [\cdot I \cdot^{(i)}] [\text{St}] V + 2k_p [\text{St}] (2\sigma_1^{(i)} + \sigma_0^{(i)}) V \\ &\quad + 2k_{tc} \sum_{j=0}^i (\sigma_0^{(i-j)} \sigma_2^{(j)} + 2\sigma_1^{(i-j)} \sigma_1^{(j)} + \sigma_2^{(i-j)} \sigma_0^{(j)}) V \\ &\quad - 2 \left(k_{fM} [\text{St}] + k_{tc} \sum_{i=0}^{\infty} (\lambda_0^{(i)} + 2\sigma_0^{(i)}) \right) \sigma_2^{(i)} V \end{aligned} \quad (29)$$

$$\begin{aligned} \frac{d(\lambda_0^{(i)} V)}{dt} &= k_{i1} [\cdot I \cdot^{(i)}] [\text{St}] V + 2k_{fM} [\text{St}] \sigma_0^{(i)} V + 2k_{tc} \sum_{j=0}^i \sigma_0^{(i-j)} \lambda_0^{(j)} V \\ &\quad + 2k_{dp} \sum_{j=i+1}^{\infty} \mu_0^{(j)} V + k_{fM} [\text{St}] \delta_{i0} \sum_{j=0}^{\infty} \lambda_0^{(j)} V \\ &\quad - \left(k_{fM} [\text{St}] + k_{tc} \sum_{j=0}^{\infty} (\lambda_0^{(j)} + 2\sigma_0^{(j)}) \right) \lambda_0^{(i)} V \end{aligned} \quad (30)$$

$$\begin{aligned} \frac{d(\lambda_1^{(i)} V)}{dt} &= k_{i1} [\cdot I \cdot^{(i)}] [\text{St}] V + k_p [\text{St}] \lambda_0^{(i)} V + 2k_{fM} [\text{St}] \sigma_1^{(i)} V \\ &\quad + 2k_{tc} \sum_{j=0}^i (\lambda_0^{(i-j)} \sigma_1^{(j)} + \lambda_1^{(i-j)} \sigma_0^{(j)}) V \\ &\quad + 2k_{dp} \sum_{j=i+1}^{\infty} \mu_1^{(j)} V + k_{fM} [\text{St}] \delta_{i0} \sum_{j=0}^{\infty} (\lambda_0^{(j)} + 2\sigma_0^{(j)}) V \\ &\quad - \left(k_{fM} [\text{St}] + k_{tc} \sum_{j=0}^{\infty} (\lambda_0^{(j)} + 2\sigma_0^{(j)}) \right) \lambda_1^{(i)} V \end{aligned} \quad (31)$$

$$\begin{aligned} \frac{d(\lambda_2^{(i)} V)}{dt} &= k_{i1} [\cdot I \cdot^{(i)}] [\text{St}] V + k_p [\text{St}] (2\lambda_1^{(i)} + \lambda_0^{(i)}) V + 2k_{fM} [\text{St}] \sigma_2^{(i)} V \\ &\quad + 2k_{tc} \sum_{j=0}^i (\lambda_0^{(i-j)} \sigma_2^{(j)} + 2\lambda_1^{(i-j)} \sigma_1^{(j)} + \lambda_2^{(i-j)} \sigma_0^{(j)}) V \\ &\quad + 2k_{dp} \sum_{j=i+1}^{\infty} \mu_2^{(j)} V + k_{fM} [\text{St}] \delta_{i0} \sum_{j=0}^{\infty} (\lambda_0^{(j)} + 2\sigma_0^{(j)}) V \\ &\quad - \left(k_{fM} [\text{St}] + k_{tc} \sum_{i=0}^{\infty} (\lambda_0^{(i)} + 2\sigma_0^{(i)}) \right) \lambda_2^{(i)} V \end{aligned} \quad (32)$$

$$\frac{d(\mu_0^{(i)} V)}{dt} = k_{fM} [\text{St}] \lambda_0^{(i)} V + \frac{1}{2} k_{tc} \sum_{j=0}^i \lambda_0^{(i-j)} \lambda_0^{(j)} V - ik_{dp} \mu_0^{(i)} V \quad (33)$$

$$\begin{aligned} \frac{d(\mu_1^{(i)} V)}{dt} &= k_{fM} [\text{St}] \lambda_1^{(i)} V + \frac{1}{2} k_{tc} \sum_{j=0}^i (\lambda_0^{(i-j)} \lambda_1^{(j)} + \lambda_1^{(i-j)} \lambda_0^{(j)}) V \\ &\quad - ik_{dp} \mu_1^{(i)} V \end{aligned} \quad (34)$$

$$\begin{aligned} \frac{d(\mu_2^{(i)} V)}{dt} &= k_{fM} [\text{St}] \lambda_2^{(i)} V + \frac{1}{2} k_{tc} \sum_{j=0}^i (\lambda_0^{(i-j)} \lambda_2^{(j)} \\ &\quad + 2\lambda_1^{(i-j)} \lambda_1^{(j)} + \lambda_2^{(i-j)} \lambda_0^{(j)}) V - ik_{dp} \mu_2^{(i)} V \end{aligned} \quad (35)$$

The average molecular weights and polydispersity can then be calculated from

$$\bar{M}_n = \frac{\sum_{i=0}^{\infty} \mu_1^{(i)}}{\sum_{i=0}^{\infty} \mu_0^{(i)}} \quad (36)$$

$$\bar{M}_w = \frac{\sum_{i=0}^{\infty} \mu_2^{(i)}}{\sum_{i=0}^{\infty} \mu_1^{(i)}} \quad (37)$$

$$D = \frac{\bar{M}_w}{\bar{M}_n} \quad (38)$$

Appendix C: Distributions module

Radical species ($i = 0, 1, \dots, n = 2, 3, \dots$)

Consider eqs (10) and (12). Assuming pseudosteady-state, all time derivatives may be set to zero and the following recurrence formulas can be obtained:

$$[\cdot S_n \cdot^{(i)}] = \frac{k_p [\text{St}] [\cdot S_{n-1} \cdot^{(i)}] + k_{tc} \sum_{j=0}^{i-1} \sum_{m=1}^{n-1} [\cdot S_{n-m} \cdot^{(i-j)}] [\cdot S_m \cdot^{(j)}]}{k_p [\text{St}] + k_{fM} [\text{St}] + k_{tc} ([R \cdot] + 2[R \cdot])} \quad (39)$$

$$\begin{aligned} [S_n \cdot^{(i)}] &= \frac{(k_p [S_{n-1} \cdot^{(i)}] + 2k_{fM} [\cdot S_n \cdot^{(i)}]) [\text{St}]}{k_p [\text{St}] + k_{fM} [\text{St}] + k_{tc} ([R \cdot] + 2[R \cdot])} \\ &\quad + \frac{2k_{tc} \sum_{j=0}^{i-1} \sum_{m=1}^{n-1} [\cdot S_{n-m} \cdot^{(i-j)}] [S_m \cdot^{(j)}] + k_{dp} \sum_{j=i+1}^{\infty} \sum_{m=n+1}^{\infty} p_{mj}(n, i) j [S_m^{(j)}]}{k_p [\text{St}] + k_{fM} [\text{St}] + k_{tc} ([R \cdot] + 2[R \cdot])} \end{aligned} \quad (40)$$

Polystyrene species ($i = 0, 1, \dots, n = 2, 3, \dots$)

The mass balances for the PS species provide

$$\begin{aligned} \frac{d}{dt} \left([S_n^{(i)}] V \right) &= k_{TM} [St] [S_n^{(i)}] V + \frac{k_{tc}}{2} \sum_{j=0}^i \sum_{m=1}^{n-1} [S_{n-m}^{(i-j)}] \\ &\quad [S_m^{(j)}] V - ik_{dp} [S_n^{(i)}] V \\ &\quad + (1-f_2)k_{dp} \sum_{j=i+1}^{\infty} \sum_{m=n+1}^{\infty} p_{mj}(n, i) j [S_m^{(j)}] V \end{aligned} \quad (41)$$

In order to account for the generation of monoradicals from random scission polymer chains by sequential decomposition of peroxide groups within the chains, consider a polymer chain with length n and i peroxide groups, all of which have the same thermal stability.

Let m be a uniformly distributed random variable whose value ranges from 1 to $n-1$. The polymer chain may form 2 monoradicals, one with length m , and the other one with length $n-m$. These chains will have $i-j$ and $j-1$ undecomposed peroxide groups respectively. If the peroxide groups are assumed to be uniformly distributed within the polymer chains in the course of polymerization, the following relation must hold:

$$\frac{j-1}{n-m} = \frac{i-j}{m} \quad (42)$$

Therefore,

$$j = \left[\frac{i(n-m) + m}{n} \right] \quad (43)$$

where the brackets indicate the integer part of the expression.

The scission has then generated two monoradicals, one with length m and $i-j$ peroxide groups, the other one with length $n-m$ and $j-1$ peroxide groups.

Note that this chain scission algorithm can be modified for specific cases. For example, in the case of a linear bifunctional initiator, since all peroxide groups are located at a chain end, $m=1$ for every scission.

The Number Chain Length Distribution (NCLD) for the PS species is

$$N_{PS}^{(i)}(n) = [S_n^{(i)}] V \quad (44)$$

found by integrating eq. (41) with eqs (39) and (40) using also eqs (9) and (11) to obtain expressions for species $[S_1^{(i)}]$ and $[S_1^{(i)}]$.

The concentration of the total PS species characterized by the number of undecomposed peroxide groups can be calculated with

$$[P^{(i)}] = \sum_{n=1}^{\infty} [S_n^{(i)}] \quad (45)$$

The NCLD for the total polymer, characterized by chain length, can be calculated using

$$P_n = \sum_{i=0}^{\infty} [S_n^{(i)}] V \quad (46)$$

The total moles of PS are

$$N_{PS} = \sum_{i=0}^{\infty} \sum_{n=1}^{\infty} N_{PS}^{(i)}(n) \quad (47)$$

To obtain the corresponding weight Chain Length Distribution (WCLD), multiply the NCLD by sM_{St} and replace n by s to obtain

$$G_{PS}^{(i)}(s) = sM_{St} [S_s^{(i)}] V \quad (48)$$

The mass of PS can then be calculated as

$$G_{PS} = \sum_{i=0}^{\infty} \sum_{s=1}^{\infty} G_{PS}^{(i)}(s) \quad (49)$$

The average molecular weights and polydispersity can then be calculated from

$$\bar{M}_n = \frac{G_{PS}}{N_{PS}} = \frac{\sum_{i=0}^{\infty} \sum_{s=1}^{\infty} G_{PS}^{(i)}(s)}{\sum_{i=0}^{\infty} \sum_{n=1}^{\infty} [S_n^{(i)}] V} \quad (50)$$

$$\bar{M}_w = \frac{\sum_{i=0}^{\infty} \sum_{s=1}^{\infty} sG_{PS}^{(i)}(s)}{G_{PS}} = \frac{\sum_{i=0}^{\infty} \sum_{s=1}^{\infty} sG_{PS}^{(i)}(s)}{\sum_{i=0}^{\infty} \sum_{s=1}^{\infty} G_{PS}^{(i)}(s)} \quad (51)$$

$$D = \frac{\bar{M}_w}{\bar{M}_n} \quad (52)$$

References

- Berkenwald, E., Spies, C., Cerna Cortez, J.R., Morales, G., Estenoz, D.A., 2013. Mathematical model for the bulk polymerization of styrene chemically initiated by sequential and total decomposition of the trifunctional initiator diethyl ketone. *J. Appl. Polym. Sci.* 128, 1–11.
- Berkenwald, E., Spies, C., Morales, G., Estenoz, D.A., 2015. Mathematical model for the bulk polymerization of styrene

- using the symmetrical cyclic trifunctional initiator diethyl ketone triperoxide. I. Chemical initiation by sequential decomposition. *Polym. Eng. Sci.* 55, 776-786.
3. Castañeda Facio, A.V., 2007. Engineering Thesis, Centro de Investigación en Química Aplicada, Mexico.
 4. Cavin, L., Rouge, A., Meyer, T., Renken, A., 2000. Kinetic modeling of free radical polymerization of styrene initiated by the bifunctional initiator 2,5-dimethyl-2,5-bis (2-ethyl hexanoylperoxy)hexane. *Polymer.* 41, 3925-3935.
 5. Cerna, J.R., Morales, G., Eyller, G.N., Cañizo, A.I., 2002. Bulk polymerization of styrene catalyzed by bi- and trifunctional cyclic initiators. *J. Appl. Polym. Sci.* 83, 1-11.
 6. Choi, K.Y., Lei, G.D., 1987. Modeling of free-radical polymerization of styrene by bifunctional initiators. *AIChE J.* 33, 2067-2076.
 7. Delgado Rodriguez, K., Morales, G., Enríquez, J., Barreto G., 2014. Presented at Macromex 2014, Nuevo Vallarta, Mexico, November.
 8. Duerksen, J.H., Hamielec, A.E., 2007. Polymer reactors and molecular weight distribution. IV. Free-radical polymerization in a steady-state stirred-tank reactor train. *J. Polym. Sci. Part C Polym. Symp.* 25, 155-166.
 9. Estenoz, D.A., Leal, G.R., Lopez, Y.R., Oliva, H.M., Meira, G.R., 1996. Bulk polymerization of styrene in the presence of polybutadiene. The use of bifunctional initiators. *J. Appl. Polym. Sci.* 62, 917-939.
 10. Galhardo, E., Magalhães Bonassi Machado, P., Ferrareso Lona, L.M., 2012. Living free radical polymerization using cyclic trifunctional initiator. *J. Appl. Polym. Sci.* 124, 3900-3904.
 11. Gonzalez, I.M., Meira, G.R., Oliva, H.M., 1996. Synthesis of Polystyrene with Mixtures of Mono- and Bifunctional Initiators. *J. Appl. Polym. Sci.* 59, 1015-1026.
 12. Hui, A.W., Hamielec, A.E., 1972. Thermal Polymerization of Styrene at High Conversion and Temperatures. An Experimental Study. *J. Appl. Polym. Sci.* 16, 749-769.
 13. Ivanov, V., Kuchanov, S., Ivanchev, S., 1977. The theory of radical polymerization with polyfunctional initiators. *Polym. Sci. USSR* 8, 1923-1932.
 14. Kim, K., Choi, K., 1989. Modeling of free radical polymerization of styrene catalyzed by unsymmetrical bifunctional initiators. *Chem. Eng. Sci.* 44, 297-312.
 15. Kuchanov, S., Ivanova, N., Ivanchev, S., 1976. Molecular weight distribution of products of radical polymerization initiated using polyfunctional initiators. *S. Polym. Sci. USSR* 8, 1870-1877.
 16. Maafa, I.M., Soares, J.B.P., Elkamel, A., 2007. Prediction of Chain Length Distribution of Polystyrene Made in Batch Reactors with Bifunctional Free-Radical Initiators Using Dynamic Monte Carlo Simulation. *Macromol. React. Eng.* 1, 364-383.
 17. Meyer, T., Keurentjes, J. (Eds.), 2005. Handbook of Polymer Reaction Engineering, Wiley, Hoboken, NJ: USA.
 18. Scheirs, J., Priddy, D., 2003. Modern Styrenic Polymers: Polystyrenes and Styrenic Copolymers, Wiley Hoboken, NJ: USA.
 19. Scolah, M.J., Dhib, R., Penlidis, A., 2006. Recent Advances in the Study of Multifunctional Initiators in Free Radical Polymerizations. *Chem. Eng. Sci.* 61, 209-221.
 20. Seavey, K.C., Liu, Y.A., Khare, N.P., Bremner, T., Chen, C.-C., 2003. Quantifying Relationships among the Molecular Weight Distribution, Non-Newtonian Shear Viscosity, and Melt Index for Linear Polymers. *Ind. Eng. Chem. Res.* 42, 5354-5362.
 21. Sheng, W.-C., Wu, J.-Y., Shan, G.-R., Huang, Z.-M., Weng, Z.-X., 2004. Free-radical bulk polymerization of styrene with a new trifunctional cyclic peroxide initiator. *J. Appl. Polym. Sci.* 94, 1035-1042.
 22. Villalobos, M.A., Hamielec, A.E., Wood, P.E., 1991. Kinetic Model for Short-Cycle Bulk Styrene Polymerization through Bifunctional Initiators. *J. Appl. Polym. Sci.* 42, 629-641.
 23. Yoon, W.J., Choi, K.Y., 1992. Free-Radical Polymerization of Styrene with a Binary Mixture of Symmetrical Bifunctional Initiators. *J. Appl. Polym. Sci.* 46, 1353-1367.